

Transport and removal of stormwater vehicle-related mobile organic contaminants in geomedia-amended sand columns

Cruz, María Alejandra; Xu, Jiaqi; Foppen, Jan Willem; Pérez, Sandra; Vázquez-Suñé, Enric; Teixidó, Marc

DOI

[10.1016/j.scitotenv.2023.164264](https://doi.org/10.1016/j.scitotenv.2023.164264)

Publication date

2023

Document Version

Final published version

Published in

Science of the Total Environment

Citation (APA)

Cruz, M. A., Xu, J., Foppen, J. W., Pérez, S., Vázquez-Suñé, E., & Teixidó, M. (2023). Transport and removal of stormwater vehicle-related mobile organic contaminants in geomedia-amended sand columns. *Science of the Total Environment*, 892, Article 164264. <https://doi.org/10.1016/j.scitotenv.2023.164264>

Important note

To cite this publication, please use the final published version (if applicable).
Please check the document version above.

Copyright

Other than for strictly personal use, it is not permitted to download, forward or distribute the text or part of it, without the consent of the author(s) and/or copyright holder(s), unless the work is under an open content license such as Creative Commons.

Takedown policy

Please contact us and provide details if you believe this document breaches copyrights.
We will remove access to the work immediately and investigate your claim.



Transport and removal of stormwater vehicle-related mobile organic contaminants in geomeedia-amended sand columns

María Alejandra Cruz^{a,c}, Jiaqi Xu^a, Jan Willem Foppen^{c,d}, Sandra Pérez^b, Enric Vázquez-Suñé^a, Marc Teixidó^{a,*}

^a Department of Geosciences, Institute of Environmental Assessment and Water Research (IDAEA), Severo Ochoa Excellence, Jordi Girona 18–26, 08034 Barcelona, Spain

^b Department of Environmental Chemistry, Institute of Environmental Assessment and Water Research (IDAEA), Severo Ochoa Excellence, Jordi Girona 18–26, 08034 Barcelona, Spain

^c Department of Water Resources and Ecosystems, IHE-Delft Institute for Water Education, Westvest 7, 2611 AX Delft, Netherlands

^d Department of Water Management, Faculty of Civil Engineering and Geosciences, Delft University of Technology, Stevinweg 1, 2628 CN Delft, Netherlands

HIGHLIGHTS

- Conventional biofilters fail to treat persistent, mobile, and toxic stormwater contaminants.
- GAC overperformed biochar in removing contaminants in geomeedia-amended sand columns.
- Removal was characterized by nonequilibrium kinetic sorption upon transport.
- GAC and biochar can retain contaminants for over a decade in 1-m depth biofilters.

GRAPHICAL ABSTRACT



ARTICLE INFO

Guest Editor: Vitor J. Vilar

Keywords:

Stormwater treatment

PMT

Nonequilibrium transport

Fouling

Pyrogenic carbonaceous materials

ABSTRACT

Green infrastructure drainage systems are innovative treatment units that capture and treat stormwater. Unfortunately, highly polar contaminants remain challenging to remove in conventional biofilters. To overcome treatment limitations, we assessed the transport and removal of stormwater vehicle-related organic contaminants with persistent, mobile, and toxic (in short: PMTs) properties, such as 1H-benzotriazole, NN'-diphenylguanidine, and hexamethoxymethylmelamine (PMT precursor), using batch experiments and continuous-flow sand columns amended with pyrogenic carbonaceous materials, like granulated activated carbon (GAC) or wheat-straw derived biochar. Our results indicated that all investigated contaminants were subjected to nonequilibrium interactions in sand-only and geomeedia-amended columns, with kinetic effects upon transport. Experimental breakthrough curves could be well described by a one-site kinetic transport model assuming saturation of sorption sites, which we inferred could occur due to dissolved organic matter fouling. Furthermore, from both batch and column experiments, we found that GAC could remove contaminants significantly better than biochar with higher sorption capacity and faster sorption kinetics. Hexamethoxymethylmelamine, with the lowest organic carbon-water partition coefficient (K_{OC}) and largest molecular volume among target chemicals, exhibited the lowest affinity in both carbonaceous adsorbents based on estimated sorption parameters. Results suggest that sorption of investigated PMTs was likely driven by steric and hydrophobic effects, and coulombic and other weak intermolecular forces (e.g., London–van der Waals, H-bonding). Results from extrapolating our data to a 1-m depth geomeedia-amended sand filter suggested that GAC and biochar could enhance the removal of organic contaminants in biofilters and last for more than one decade. Overall, our work is the first to study treatment alternatives for NN'-diphenylguanidine and hexamethoxymethylmelamine, and contributes to better PMT contaminant removal strategies in environmental applications.

* Corresponding author.

E-mail address: marc.teixido@idaea.csic.es (M. Teixidó).

1. Introduction

Urban stormwater has long been managed only to reduce flood risks. However, stormwater is increasingly viewed as an asset to augment local water supplies (Luthy et al., 2019). With drought and flood events becoming more severe and frequent, stormwater harvesting represents a unique opportunity to effectively build climate change resilience in urban environments. In this context, non-traditional innovative drainage systems, such as green infrastructure, are increasingly built to capture and treat urban stormwater while providing multiple environmental and societal benefits for urban dwellers (Batalini de Macedo et al., 2021). However, stormwater can carry over 600 pollutants, mainly from vehicle-related sources (Eriksson et al., 2007), and conventional green infrastructure (including biofilters) fail to remove the polar (i.e., mobile) contaminant fraction (Spahr et al., 2020; Teixidó et al., 2022). These contaminants generally exhibit logarithmic organic carbon-water partition coefficients ($\log K_{OC}$) or logarithmic octanol-water distribution coefficients ($\log D_{OW}$) below 3, at circumneutral pH values; meaning they are mobile substances (i.e., “M” in the PMT acronym) (Arp and Hale, 2019), they adsorb weakly onto soil constituents (Reemtsma et al., 2016), and can ultimately reach different water bodies.

Among the vehicle-related organic contaminants, *NN*-diphenylguanidine (DPG), 1H-benzotriazole (BTZ), hexamethoxymethylmelamine (HMMM), and their transformational products are currently under the spotlight due to their detection in storm-, ground-, and drinking water (Peter et al., 2018; Schulze et al., 2019; Hinnenkamp et al., 2022), their recalcitrance in treatment facilities (Farré et al., 2008; Schulze et al., 2019), and their recently found ecotoxicological risks (Johannessen et al., 2021; Sandré et al., 2022). Furthermore, both DPG (tire wear particle leachate) and BTZ (corrosion inhibitor) have been identified as prioritized persistent, mobile, and toxic (PMT) and very persistent and very mobile (vPvM) substances (Category 1; priority substances for follow-up) (Arp and Hale, 2019). Although HMMM (tire wear particle leachate) is not strictly considered a PMT/vPvM contaminant, Wiener and LeFevre (2022) identified the prioritized PMT/vPvM substance melamine as a plausible “dead-end” product of HMMM biotransformation.

Therefore, these PMT vehicle-related organic contaminants in stormwater inevitably reach conventional biofilters and percolate through, potentially contaminating groundwater. Amendments with pyrogenic carbonaceous materials (PCMs) such as (regenerated) activated carbon and biochar have proven to remove several dissolved ionizable and ionic organic contaminants in stormwater during passive infiltration (Ray et al., 2019; Spahr et al., 2020; Teixidó et al., 2022); involving several drivers and interactions: hydrophobic (solvophobic) and steric effects, coulombic and London–van der Waals forces, π - π electron donor-acceptor (EDA) and H-bonding interactions (Teixidó et al., 2011; Xiao and Pignatello, 2015; Tong et al., 2019). Research has determined factors that can significantly impact biofilter media performance and durability, such as the physicochemical properties of sorbents (e.g., elemental composition, surface activity, porosity) and runoff composition (e.g., nutrients, inorganic salts, organic pollutants, dissolved organic carbon, pH) (Esfandiari et al., 2022). Sorption capacity generally increases with PCM production temperature, pore volume, and surface area (Lattao et al., 2014; Tong et al., 2019). The sorbents particle size would also influence sorption by changing the intraparticle kinetic diffusion (e.g., shortening internal paths to sorption sites) (Boehm et al., 2020). However, to our knowledge, no studies have assessed the potential removal of DPG and HMMM contaminants by PCMs in stormwater (in)filtration systems.

The effects of PCMs on organic contaminant transport in porous media treating stormwater have been widely studied for hydrophobic compounds but less for polar compounds (Ulrich et al., 2015). Sorption is often simplified and assumed to reach instantaneous equilibrium (i.e., equilibrium transport) (Guelfo et al., 2020). However, mass transfer between sorbing organic contaminants and porous adsorbents may be rate-limited (de Wilde et al., 2008; Brusseau et al., 2019; Hossain

and McLaughlan, 2021) (i.e., with nonequilibrium transport), mainly because of intraparticle diffusion (Werner et al., 2012).

Rate-limited sorption can have important implications for the transport and fate of chemicals in the infiltrating medium (Chen et al., 2019; Guelfo et al., 2020; Hossain and McLaughlan, 2021). The importance of nonequilibrium processes in the sorption of contaminants is a function of the physical properties of the sorbents, the nature of the chemical interactions, and pore water flow velocity (Mao and Ren, 2004). For example, the kinetic effects on transport intensify with higher flow velocities and shorter distances (Werner et al., 2012), making it especially relevant in shallow infiltration systems (Ulrich et al., 2015). In one-dimensional (1-D) flow-through column experiments, nonequilibrium processes result in early solute breakthrough and/or asymmetrical breakthrough curves (Guelfo et al., 2020).

Understanding the rate-limited transport of contaminants allows us to predict removal performance and optimize design options of geomediamended biofilters (Tong et al., 2019). Thereto, this work aimed to evaluate the potential of different PCMs to enhance the removal of the PMT vehicle-related stormwater contaminants (BTZ, DPG, and HMMM) in geomediamended passive infiltration systems and study their transport behavior. To this end, we conducted lab-scale batch and column experiments (using realistic infiltration rate, dissolved organic matter, and biologically active conditions) with different geomediamedia to identify the best candidate amendment material. In addition, we applied a 1-D model to fit nonequilibrium sorption and quantify transport parameters. Finally, we extrapolated the results for a 1-m depth column to estimate the service life of a biofilter under conditions likely encountered in a maritime Mediterranean climate city (Barcelona, Spain).

2. Methods

2.1. Materials

2.1.1. Pyrogenic carbonaceous materials

Fourteen PCMs were initially screened, including Jacobi Carbons (Merseyside, United Kingdom) commercially available fresh granulated activated carbon (GAC) and regenerated activated carbon (RAC). For the reactivation of exhausted activated carbon (RAC) performed at Jacobi facilities (France), the spent material from drinking water treatment plants was pre-dried at 120 °C, separated from impurities by density, thermally reactivated at around 700 °C in a controlled atmosphere, sieved to restore its initial granulometry, and complemented with fresh GAC to compensate for losses in the regeneration cycle. In addition, twelve standard biochars (known as the “Edinburgh Standard Biochar set”) produced by the United Kingdom Biochar Research Centre (UKBRC) at the University of Edinburgh (United Kingdom) were used (Mašek et al., 2018). All PCMs were gently crushed with a mortar and sieved to a 0.5–0.85 mm particle size range. The same particle size range as the main packing column material (i.e., silica sand) was used to avoid geomediamedia losses throughout the column experiment.

The summary of the PCM physicochemical characteristics is provided in the Supplementary materials (Table S1). The geomediamedia surface areas were determined by Brunauer-Emmett-Teller (B.E.T.) analysis with N_2 adsorption at 77 K. Only the biochar with the highest mean removal during the batch material initial screening (i.e., biochar derived from wheat straw pellets pyrolyzed at 550 °C; WSP550) and the commercial GAC for performance benchmark were used further in the study. The biochar N_2 B.E.T. surface area of $6.09 \text{ m}^2 \text{ g}^{-1}$ and GAC surface area of $878 \text{ m}^2 \text{ g}^{-1}$ indicated a notable difference between them. Although the specific surface area of the Edinburgh Standard Biochar set fell within the low range of reported values for PCMs (Tomczyk et al., 2020; Teixidó et al., 2013), they enabled reproducible results.

2.1.2. Synthetic stormwater

All experiments were carried out with synthetic stormwater prepared from deionized water and salts (i.e., CaCl_2 , MgCl_2 , NH_4Cl , Na_2SO_4 , NaHCO_3 , NaNO_3 , and NaH_2PO_4 ; Table S2) to obtain total carbonate,

nitrogen and phosphorus concentrations representative of urban runoff (Grebel et al., 2013), at 5 mg C L⁻¹ dissolved organic carbon (DOC) and pH of 6.5. Sigma-Aldrich humic acid was only used in the preliminary batch screening experiments. Representative DOC concentrated stock (1 g C L⁻¹) was used for most of the experiments and was prepared based on Ulrich et al. (2015) with 15 L of deionized water equilibrated for a fortnight at room temperature with 80 g of dry leaves, 150 g of grass, 670 g of plant-based compost, and 300 g of straw. This organic matter tea was filtered (glass fiber filter, 0.7 µm), stored in amber bottles, and frozen (-4 °C) until use. Sodium azide (NaN₃) ranging from 1.5 to 3.1 mM was added to the matrix.

2.2. Batch experiments

2.2.1. Material screening

The PCM screening was conducted to identify which biochar exhibited the highest sorption towards the three studied vehicle-related contaminants and to determine the optimum solid-to-liquid ratio. Different solid-to-liquid ratios were employed by adding 5 mg, 10 mg, and 25 mg of PCMs in 50 mL of synthetic stormwater (corresponding to 0.1, 0.2, and 0.5 g sorbent L⁻¹, respectively). Synthetic stormwater was prepared with 5 mg C L⁻¹ DOC (Sigma-Aldrich humic acid), 1.5 mM NaN₃, and spiked with 0.3 µM of the contaminants, such that the final methanol concentration was below 0.5 % (Teixidó et al., 2011). The geomeedia was pre-equilibrated with synthetic stormwater for 24 h before the contaminant spike, and it was followed by a short equilibration time of 5 days. During the experiment, reactors were placed on an end-over-end rotary shaker at 10 rpm. Controls were used with and without sorbent material to monitor the effects of PCM-induced pH changes and to account for the reactor losses (<6 %), respectively.

The distribution coefficient (K_d , L kg⁻¹) was calculated as the ratio between the sorbed (q) and liquid-phase (C_e) concentrations:

$$K_d = \frac{q}{C_e} = \frac{V}{M_s} \cdot \frac{(C_0 - C_e)}{C_e} \quad (1)$$

where q (mg kg⁻¹) is the sorbed concentration, C_e (mg L⁻¹) is the liquid-phase concentration, C_0 (mg L⁻¹) is the liquid-phase concentration in the control (without sorbent), V (L) is the liquid volume, and M_s (kg) is the sorbent mass.

2.2.2. Adsorption kinetics

Batch kinetic experiments were carried out in triplicate for each contaminant to study sorption rates onto GAC and WSP550 biochar. Reactors contained 50 mL of synthetic stormwater, prepared with 5 mg C L⁻¹ of DOC (from the 1 g C L⁻¹ concentrated stock) and 3.1 mM NaN₃. After 24 h of pre-equilibration with 25 mg of PCM (except GAC for BTZ and DPG, using 5 mg and 10 mg, respectively), 0.3 µM of contaminants were added. Batch vials were agitated in an end-over-end rotary shaker at 10 rpm, and pH was monitored daily to control changes (control with sorbent). Controls without sorbent were used to track reactor losses (<6 %) and used as initial concentrations. For sample collection, aliquots were taken at pre-selected intervals within seven days (at 3, 6, 12, 24, 48, 72, 120, and 168 h). The sorbed concentration (q) was determined by mass balance, and kinetics data were fitted to pseudo-first-order (PFO) (calculations in SI), commonly used to describe the adsorption kinetics of contaminants on carbon-based sorption materials (Xiao et al., 2017). The equation for the PFO model is as follows:

$$\frac{dq_t}{dt} = k_1(q_e - q_t) \quad (2)$$

where q_t and q_e are the adsorbed contaminant concentration at time t and at equilibrium (mg kg⁻¹), t is time (h), and k_1 (kg mg⁻¹ h⁻¹) is the PFO kinetic rate constant.

The adsorbed concentration at equilibrium and the rate constant were solved using the GraphPad Prism software based on the least square error between experimental and modelled values.

2.3. Column experiment

2.3.1. Column system setup

Ten continuous-flow columns were used to assess the removal performance of the PCM (GAC or biochar) towards the selected vehicle-related organic contaminants and their transport in simulated field conditions. A first set of columns was operated under biotic conditions, while a second group flowed under abiotic conditions (Fig. 1). The PVC columns (19.5 cm in length, 3.2 cm inner diameter) were packed with commercial silica sand (AXTON SiO₂), sand amended with GAC, and sand amended with WSP550 biochar (all materials at 0.5–0.85 mm range). The column diameter to particle size ratio exceeded the minimum recommended (40) to limit boundary effects (Gibert et al., 2014). Gravels commonly used in green infrastructure setups in the City of Barcelona (Spain) were packed at the top and bottom of the column (1 cm of coarse gravel: >1.7 mm, and 1.75 cm of finer gravel: 0.5–1.7 mm) to support and secure the 14 cm portion of reactive material-amended sand. The sand and gravel were acid-washed with 5 % HNO₃ to remove impurities (e.g., metals and carbonates) and then thoroughly rinsed with deionized water until neutral pH was obtained.

GAC and biochar were added at 0.5 wt% to the sand and gently mixed prior to column packing. In addition, all columns contained 1 wt% of sand extracted from an existing bioswale (i.e., solid inoculum), previously autoclaved for the abiotic set of columns. This low percent-by-weight of reactive geomeedia (GAC and biochar) allowed the observation of PMT contaminant transport throughout the experiment. Besides, stormwater biofilters should not be amended with high percentages of carbon-based materials as they could compromise their hydraulic properties (Boehm et al., 2020). Columns were dry-packed, mechanically shaken to maximize packing density, and flushed with CO₂ gas in up-flow direction right before start-up to ensure water saturation. The porosity of the columns was estimated gravimetrically after water saturation and corrected to subtract the porosity in the gravel layers.

The ten columns operated up-flow mode at a volumetric flow rate of 1.84 ± 0.1 mL min⁻¹ (5.5 cm h⁻¹ linear velocity) by means of two multi-channel peristaltic pumps. The flow rate was defined based on the recommended design for biofilters to treat urban runoff (Ekka et al., 2021). Tracer tests with 90 mM NaCl were carried out to estimate the mean hydraulic residence time and examine the breakthrough curve for each column type.

2.3.2. Conditioning stage

Previous to contaminant injection, 100 pore volumes (PVs) of a microbe-enriched solution (liquid inoculum) were flushed through the biotic columns in a closed circuit to promote microbial attachment. The same solution with 6.2 mM NaN₃ was injected into the abiotic control columns. This liquid inoculum was prepared with 2.4 L of deionized water, 0.14 mM of lactate, and equilibrated for 15 days with 20 wt% of sand collected from an existing bioswale. The solution was intermittently aerated and, before its injection, it was filtered (glass fiber filter, 0.7 µm) and diluted with Milli-Q water until reaching <1 mg C L⁻¹ DOC. Finally, the columns were conditioned for 100 PVs with contaminant-free synthetic stormwater (5 mg C L⁻¹ of DOC concentrated stock; 3.1 mM NaN₃ in the abiotic set) for DOM pre-exposure and to remove pyrolyzed fines from the system before contaminant spike.

2.3.3. Contaminant challenge test

After the columns were conditioned, they were challenged with BTZ, DPG, and HMMM spiked synthetic stormwater (0.3 ± 0.05 µM initial concentration) over 600 PVs (Fig. S3). Relatively high concentrations of contaminants, compared to reported concentrations in stormwater and surface waters (e.g., BTZ: 0.05 µM — Giger et al., 2006; DPG: 0.01 µM — Peter et al., 2018; and HMMM: 0.03 µM — Johannessen et al., 2021),

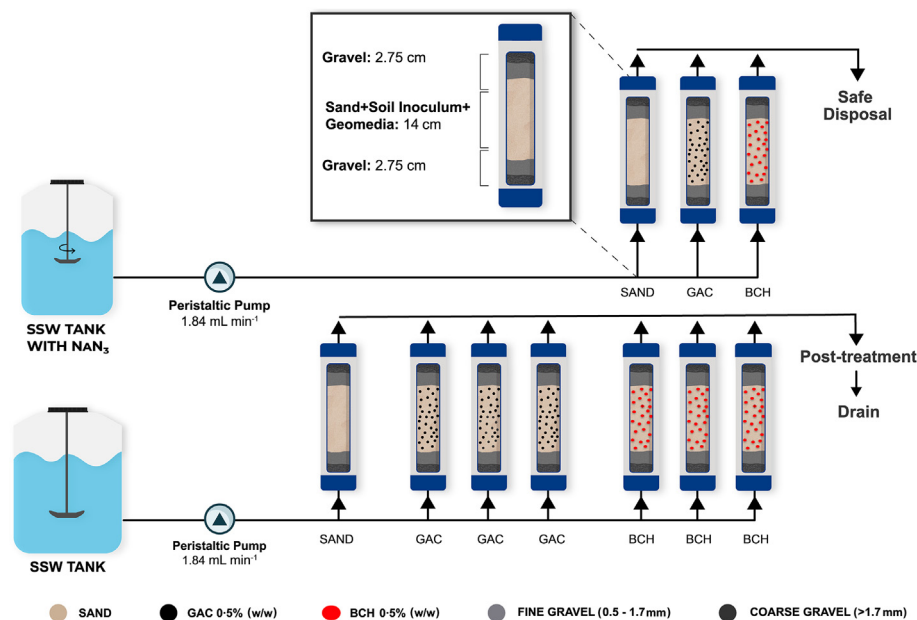


Fig. 1. Schematic representation of the column experiment system run at $1.84 \pm 0.1 \text{ mL min}^{-1}$. Two different synthetic stormwater (SSW) influents were assessed: with (on the top) and without azide (on the bottom), to represent biotic and abiotic environments, respectively. PVC columns were dry packed with sand, sand amended with 0.5 wt% activated carbon (GAC), and sand amended with 0.5 wt% WSP550 biochar (BCH) and secured with gravel supports at the top and bottom of the columns.

were spiked to produce breakthroughs within the time frame of the experiment. However, concentrations in stormwater above $1.4 \mu\text{M}$ have been reported (Challis et al., 2021). The adopted term ‘challenge test’ implies testing a stormwater treatment system under extreme conditions (Zhang et al., 2014). Information on the contaminant CAS number, molecular structure, suppliers, and other details, can be found in Tables 1 and S3 (chemicals were used as received). Methanol in the contaminants stock mix was evaporated (to avoid excessively high DOC concentrations at the column effluents), and the dried mix was redissolved in deionized water before its application.

Influent reservoirs were stirred with a PTFE impeller and prepared every three days to minimize contaminant (bio)transformation and microbial growth. Weekly analyses of influent and effluent samples for standard water quality indicators (i.e., pH, temperature, electric conductivity,

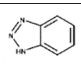
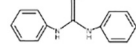
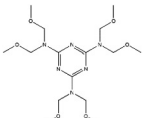
dissolved oxygen, DOC) were used to measure overall column performance. Samples to analyze organic contaminants concentrations were taken regularly from the influent tanks to ensure constant levels and account for possible variations.

2.4. Analytical methods

Trace organic contaminants were quantified by Ultra High-Performance Liquid Chromatography (UPLC), coupled with XEVO TQ-S triple quadrupole tandem Mass Spectrometer (LC-QqQ-MS/MS, Waters Corporation). The mass spectrometer was operated in positive and negative electrospray ionization (ESI), with multiple reaction monitoring, acquiring two transitions (i.e., one quantifier and one qualifier) for each analyte. Separation for chromatography was performed at 40°C

Table 1

Target stormwater vehicle-related contaminants of emerging concern. Physicochemical properties, PMT criteria, and common sources in stormwater.

Name (acronym, CAS)	Molecular structure	M_w (g mol^{-1}) and V_m (\AA^3) ^a	$\text{Log } K_{OC}$ ^b	$\text{Log } D_{OW}$ (pH 7.4) ^c	$\text{Log } S_w$ (mg L^{-1}) ^b	PMT/vPvM criteria ^d	Source and references
1H-Benzotriazole (BTZ, 95–14-7)		119.12/77.00	3.00	1.28	3.78	YES (category 1)	Corrosion inhibitor ^g
NN'-Diphenylguanidine (DPG, 102-06-7)		211.11/141.39	3.77	1.28	3.22	YES (category 1)	Vulcanisation accelerator ^h
Hexamethoxy-methylmelamine (HMMM, 3089-11-0)		390.22/331.44	1.00	2.45	2.17	Potential precursor (category 1) ^{e,f}	Cross-linking agent ⁱ

^a Van der Waals molecular volume calculated using Perkin Elmer Chem3D software.

^b Logarithmic K_{OC} and water solubility (S_w) at 25°C generated from US Environmental Protection Agency EPISuite™.

^c Logarithmic D_{OW} values at pH 7.4 calculated using ACDlabs.com ACD/LogD.

^d PMT/vPvM criteria together with REACH emission likelihoods given by Arp and Hale (2019).

^e Melamine is a PMT/vPvM substance (Category 1) and it is considered a “dead-end” transformation product for HMMM.

^f Similar structure to triazine compounds with sublethal consequences in organisms suggests HMMM (and derivatives) toxicity cannot be underestimated (Johannessen et al., 2021).

^g Sandré et al. (2022).

^h Müller et al. (2022), Peter et al. (2018), and Seiwert et al. (2020).

ⁱ Johannessen and Parnis (2021) and Johannessen et al. (2021).

at a flow rate of $0.350 \text{ mL min}^{-1}$, using an Acquity UPLC HSS T3 (Waters, $2.1 \times 10 \text{ mm}$, $1.8 \mu\text{m}$) chromatography column and a water-methanol gradient containing 5 mM of Sigma-Aldrich ammonium formate (for details on the analytical method, gradient profile, and instrumental detection limits see Tables S4 and S5). Analyte quantification was based on the chromatography-mass spectrometer parameters from analytical standards, using an external matrix-matched calibration curve to correct the ionization influence of the matrix (Buhrman et al., 2008). All samples were filtered with cellulose acetate syringe filters ($0.45 \mu\text{m}$) and injected with the deuterated internal standard mix at $10 \mu\text{g L}^{-1}$.

Standard water quality indicators pH, temperature, and electric conductivity were evaluated with a Hach multiparameter probe. Dissolved oxygen (DO) concentrations in column effluents were determined by employing an air-tight flow cell connected to the column effluent, leaving 30 min between lectures to obtain a stable DO reading. Samples for DOC were filtered with polyvinylidene difluoride membrane syringe filters ($0.45 \mu\text{m}$), acidified with HNO_3 until reaching a pH value of $2\text{--}3$, and measured with a Shimadzu Total Organic Carbon Analyzer (TOC-VCSH).

2.5. HYDRUS 1-D transport model

The breakthrough curves for the NaCl tracer experiment were fitted with a numerical solution to the advection-dispersion equation, using the equilibrium model in the open source HYDRUS 1-D software and the soil hydraulic parameters of the columns, previously estimated gravimetrically (0.4 saturated water content; 0.29 cm min^{-1} saturated hydraulic conductivity, Table S6). The dispersivity was determined from the best fit and then utilized for modelling organic contaminants transport. Experimental data was adjusted to subtract hold-up time outside the (reactive) sand section.

Various models have been developed to describe rate-limited sorption with nonequilibrium transport in the porous media. In this work, the nonequilibrium HYDRUS one-site transport model assuming Langmuirian dynamics was fitted to the experimental contaminant breakthrough data to account for the blocking of sorption sites (i.e., NOM fouling). Sorption parameters (i.e., attachment coefficients and S_{max}) were optimized using the Levenberg-Marquardt algorithm (least squares method).

The one-dimensional nonequilibrium chemical transport and the fate of solutes with the advection-dispersion equation and the mass balance transfer between aqueous and solid kinetic phases can be described as:

$$\theta \frac{\partial C}{\partial t} + \rho_b \frac{\partial q}{\partial t} = \frac{\partial}{\partial x} \left[\theta D \frac{\partial C}{\partial x} \right] - \frac{\partial fC}{\partial x} \quad (3)$$

$$\rho_b \frac{\partial q}{\partial t} = \theta k_a \psi C - k_d \rho_b q \quad (4)$$

where C is the concentration in the aqueous phase (g cm^{-3}), q is the concentration in the solid phase (g g^{-1}), t is time (min), θ is the volumetric water content ($\text{cm}^3 \text{ cm}^{-3}$), ρ_b is the dry bulk density (g cm^{-3}), D is the dispersion coefficient ($\text{cm}^2 \text{ min}^{-1}$), f is the volumetric fluid flux density (cm min^{-1}), and x is the vertical coordinate positive upward (cm). k_a is the first-order attachment coefficient (min^{-1}), and k_d is the first-order detachment coefficient (min^{-1}). Finally, ψ is a dimensionless blockage function that can simulate the decrease in the attachment coefficient due to the filling of favorable sorption sites (S_{max}) and can be described following the Langmuirian dynamics equation (Šimůnek et al., 2018):

$$\psi = 1 - \frac{S}{S_{\text{max}}} \quad (5)$$

2.5.1. Simulation of service life

Using the optimized model parameters, breakthrough results were extrapolated to a 1-m depth geomedia-amended sand column to simulate and approximately predict the service life of one biofilter in Barcelona

City (Fig. S4). The simulated unit was assumed to be 5 m^2 with 180 m^2 of capture area (100% impervious), where annual precipitation (592 mm) produces on average 100 m^3 of road runoff per year, loaded with 2.55 mmol (1 g) of HMMM. The lifetime was defined at the 50% breakthrough of the most mobile target contaminant (i.e., HMMM) (further information in the Suppl. materials).

3. Results and discussion

3.1. Batch sorption experiments

The preliminary batch screening tests (i.e., single- K_d experiments) revealed that the 5-day distribution coefficients ($\log K_d$) for the fourteen evaluated PCMs ranged from 2.18 to 3.40 L kg^{-1} (Table S7). Activated carbons (i.e., GAC and RAC) exhibited the highest $\log K_d$ values as observed in previous studies (Spahr et al., 2022). Regarding biochars, WSP550 showed the highest removal, achieving $\log K_d$ values similar to the commercial chars (i.e., differences below $0.5 \log$ units), though its $\text{N}_2 \text{ B.E.T.}$ surface area was not the largest. In addition, no correlations between 5-day $\log K_d$ values and other PCM physicochemical properties were observed. Only the WSP550 biochar and the GAC (performance benchmark) were used further in this study. BTZ and DPG showed higher removal than HMMM among these two adsorbents.

Kinetic curves for DPG, BTZ, and HMMM adsorption onto the biochar and GAC are depicted in Fig. 2 (additional results in Table S8). Sorbed concentrations (q) increased with time and, in most cases, attained quasi-conditions of equilibrium by the end of the experiment. However, after five days of reaction, BTZ and HMMM did not reach sorption equilibrium in biochar reactors. The studied biochar exhibited slower contaminant uptake rates, reaching a plateau (adsorption $>90 \%$) for BTZ and DPG after approximately 168 h of reaction ($k_1 = 0.030 \text{ h}^{-1}$ for BTZ and 0.029 h^{-1} for DPG). In contrast, sorption onto GAC reached similar high adsorption levels after only 24 h ($k_1 = 0.254 \text{ h}^{-1}$ for BTZ and 0.193 h^{-1} for DPG), indicating adsorption kinetics onto GAC were around seven times faster. HMMM presented the lowest kinetic rate constants in both adsorbents ($k_1 = 0.062 \text{ h}^{-1}$ for GAC and 0.010 h^{-1} for WSP550 biochar). Regarding q_e values, results confirmed that GAC exhibited the highest sorption capacity (i.e., mmol kg^{-1}), which could lead to higher attenuation performance (i.e., removal) in a potential PCM-amended biofilter.

3.2. Column experiments

3.2.1. Columns performance

The column testbed successfully operated throughout the entire experiment. NaCl tracer test results and hydraulic retention times (HRT) of the columns are provided in Fig. S2 and Table S9. The results showed the 50% breakthrough point at 1 PV , reaching the unity of relative concentration (i.e., C/C_0) before the second pore volume. The shape of the conservative tracer breakthrough curve confirmed the adequate setup and the absence of preferential flow paths in all the columns. Experimental data fit with HYDRUS inverse modelling yielded a mean HRT of 23.4 min and an optimized dispersivity value of 0.15 cm . The obtained Peclet numbers above unity indicated advection dominant transport.

In the biotic columns, throughout the experiment, the average DOC removal consistently decreased (from 30 to 17%), while DO removal increased (from 21 to 34%) (Fig. 3). In the abiotic columns, DOC removal decreased from 22 to 6% . A simplified mass balance of DOC removal at the initial and last stage of the challenge test (Fig. 3a) indicated that the adsorption capacity of the PCM likely governed initial removal, as it was higher in the PCM amended columns. However, the contribution of biologically enhanced removal had grown by the end of the test. The relatively high DOC removal, regardless of the drop in the DOC adsorption capacity by the carbonaceous adsorbents (i.e., fouling), along with the higher DO depletion (Fig. 3b), suggested an increased biological activity (i.e., respiration). Similar column performance evolution (DOC and DO)

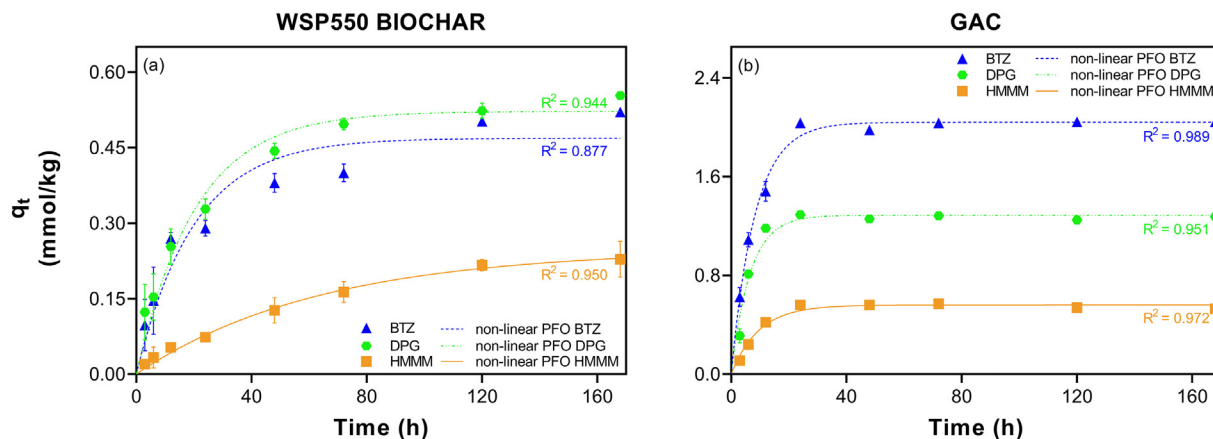


Fig. 2. Batch kinetics results (symbols) and fitted pseudo-first-order (PFO) model (lines) for BTZ, DPG, and HMMM adsorption onto WSP550 biochar (a) and GAC (b), using a synthetic stormwater matrix spiked at $0.3 \mu\text{M}$ (initial contaminant concentration) and a solid-to-liquid ratio of 0.5 g L^{-1} ; except for BTZ (0.1 g L^{-1}) and DPG (0.2 g L^{-1}) in GAC-containing reactors. Error bars indicate standard deviation from triplicates. The sorbed concentration at equilibrium (q_e) and kinetic rate constant (k_1) parameters estimated from the fit to the PFO model are included in the Suppl. materials (Table S8).

has been observed in both lab- and field-scale column experiments studying the removal of stormwater contaminants by similar sorptive carbon-based materials (Spahr et al., 2022; Teixidó et al., 2022). Based on the DO measurements at the column effluents, columns remained above $1 \text{ mg O}_2 \text{ L}^{-1}$ during the experiments.

3.2.2. Contaminant breakthrough curves

At 600 PVs, the sand-only columns (Fig. 4a-c) exhibited low removal and no significant differences between biotic and abiotic conditions results of BTZ, DPG, and HMMM ($p > 0.05$, 2-way ANOVA, Tukey post hoc test, Tables S11-S13). Contaminants completed breakthrough after a plateau phase that progressively increased following a steep initial slope. The relative concentrations (C/C_0) of 0.8 (DPG) and 0.9 (BTZ and HMMM) at 10 PVs in sand-only columns emphasized the poor removal this widely applied biofilter material provides for the target polar vehicle-related organic contaminants.

Similarly, biochar-amended column breakthrough curves of biotic and abiotic conditions (Fig. 4d-f) had no significant statistical differences ($p > 0.05$, 2-way ANOVA, Tukey post hoc test, Tables S11-S13). Samples at 10 PVs with C/C_0 values of BTZ, DPG, and HMMM, between 0.6 and 0.8, indicated that the contaminant breakthrough occurred with a sharp initial slope. The C/C_0 increased steadily in the biochar-containing columns until they reached unity for all three contaminants after 500 PVs. For the short HRT we used, no significant differences could be found between

removal of organic contaminants in sand-only and WSP550 biochar-amended columns ($p > 0.05$, 2-way ANOVA, Tukey post hoc test, Tables S11 and S12).

The biotic and abiotic conditions in GAC-containing columns resulted in negligible differences, except for the BTZ removal ($p < 0.05$, 2-way ANOVA, Tukey post hoc test, Tables S11-S13), where biologically enhanced might have contributed to some 9 % of BTZ removal on average (calculated by mass balance; Fig. 5). Nonetheless, breakthroughs of the three contaminants in these GAC-amended filters followed the same general shape, with a steep rise followed by a plateau of gradually increasing relative concentrations. The C/C_0 for BTZ (Fig. 4g) and DPG (Fig. 4h) remained lower than 0.6 after 600 PVs and about 100 PVs for HMMM (Fig. 4i). Compared to sand-only and biochar-amended columns, the lower C/C_0 values indicated that GAC-amendments removed contaminants significantly better ($p < 0.05$, 2-way ANOVA, Tukey post hoc test, Tables S11 and S12).

The breakthrough curves in Fig. 4 showed that equilibrium between dissolved and adsorbed fractions of the organic pollutants did not occur instantaneously and suggested the presence of nonequilibrium processes. The observed general shape of a steep initial rise followed by a plateau phase that slowly increased in all the columns was typical of kinetic transport (Guelfo et al., 2020). The plateau phase occurred at different relative concentrations (C/C_0) between packing materials following the sequence of sand (0.8–0.9), biochar-amended (0.6–0.8), and GAC (0.2–0.6). But, by

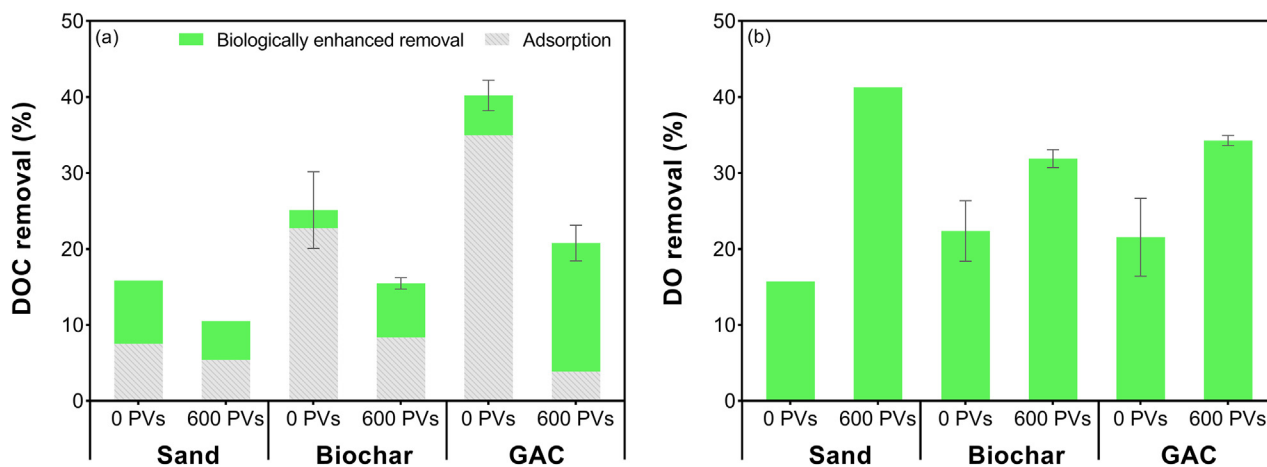


Fig. 3. Removal percentage of (a) DOC and (b) DO in the biologically active columns from effluent samples taken after the conditioning stage (0 PVs), and at the end (600 PVs) of the contaminant challenge test (Fig. S3). Subtraction of the DOC removal in biologically active columns from the DOC removal in abiotic columns (i.e., DOC adsorption) yielded the biologically enhanced removal values. Error bars indicate standard deviation of the results from three replicated biotic columns.

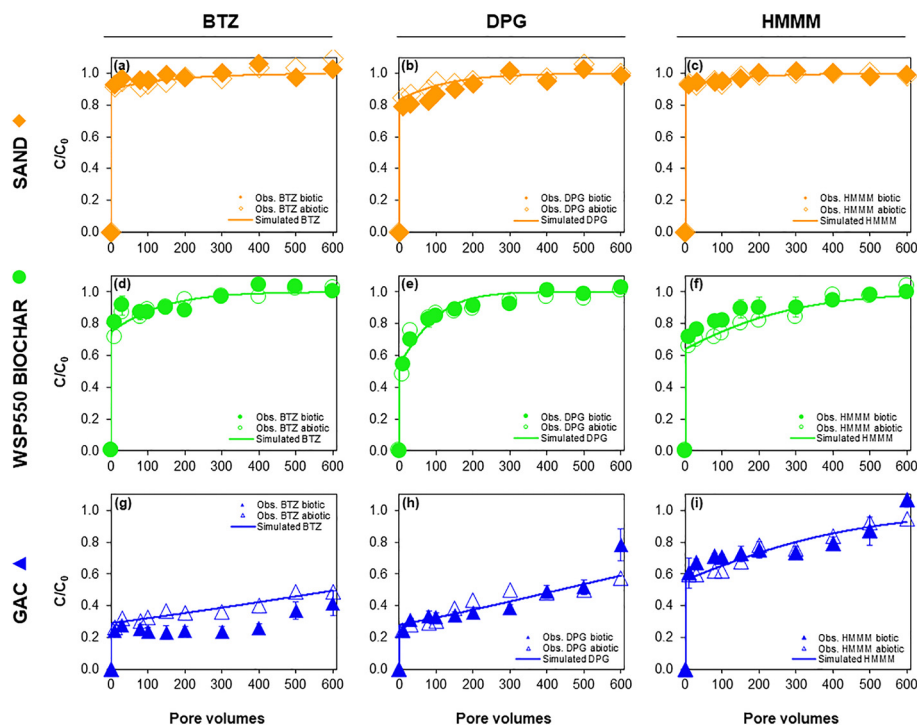


Fig. 4. Experimental column breakthrough curves (symbols) and fitted HYDRUS one-site transport model assuming Langmuirian dynamics (lines) for DPG, HMMM, and BTZ adsorption onto sand-only (a-c), biochar-amended (d-f), and GAC-amended (g-i) sand columns. The test was conducted using synthetic stormwater spiked at $0.3 \pm 0.05 \mu\text{M}$ (initial contaminant concentration) for over 600 pore volumes following 100 pore volumes of microbial seeding and 100 pore volumes of conditioning with contaminant-free synthetic stormwater. Error bars indicate standard deviation from column triplicates.

the end of the experiment, contaminants breakthroughs were complete, except for BTZ ($C/C_0 = 0.4\text{--}0.5$) and DPG ($C/C_0 = 0.6$) in GAC-amended columns. Rate-limited diffusion was likely intensified by the column composition (i.e., a homogenous mix of sand with 0.5 wt% of geomedia) and governed the contaminant sorption process in the column testbed. Hence, breakthroughs in treatment units operating under equilibrium conditions (Hossain and McLaughlan, 2021) or packed with 100 %

geomedia (e.g., GAC filters used for drinking water treatment) would differ notoriously from our results.

In this study, the biological removal of DPG (PMT) and HMMM (PMT precursor) seemed negligible. The results of DPG agreed with its reported high persistence in the environment (Müller et al., 2022); however, Alhelou et al. (2019) found that HMMM continuously biotransforms in surface and subsurface water into more persistent and mobile compounds. The only contaminant subject to biologically enhanced removal (i.e., biotransformation or biologically enhanced sorption) was BTZ (9 % calculated contribution to removal on average), which has been reported to biotransform by Liu et al. (2011) and Ulrich et al. (2017). Unfortunately, our results do not allow any firm mechanistic conclusions over the biotic contribution to BTZ removal. While identifying transformation products was beyond the scope of this study, it is deemed necessary to assess the removal of the contaminants in the column system and study the involved mechanisms. Besides, it would provide more information for evaluating the removal of upgraded biofilters and the potential risk of leaching (bio) transformation products into the environment.

3.2.3. Modelling transport with HYDRUS

All contaminant breakthrough curves could be well-fitted with the non-equilibrium one-site transport model with blockage of sorption sites (Fig. 4). Similar goodness of fit was observed with RMSE and Pearson correlation coefficient (R^2 ranging from 0.81 to 0.95; Table S14), except for the BTZ data in sand-only columns, which underestimated C/C_0 values between 400 and 600 PVs and produced the lowest Pearson R^2 value of all the models (0.66). Minor discrepancies with the experimental breakthrough curve of BTZ were likely caused by the remobilization of the contaminant previously absorbed in the system, as previously observed in biochar-augmented bioreactors (Ashoori et al., 2019).

Model parameters (summarized in Table S14) indicated that attachment coefficients (k_a) were lowest in the sand, followed by biochar and GAC. The maximum normalized favorable sorption sites ($S_{\text{max}}^* = S_{\text{max}}/C_0$) was also the lowest in sand-only columns and increased by one order

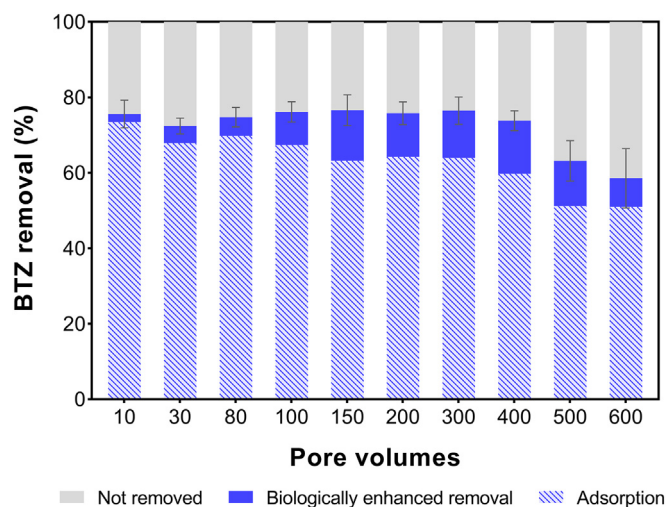


Fig. 5. Mass balance of BTZ enhanced removal in GAC amended columns. The sorption contribution at each pore volume was estimated from the difference between the unity and the removal in the abiotic GAC-amended columns. The difference between the sorption contribution and the average enhanced removal in the biologically active GAC-amended columns yielded the share of biologically enhanced removal. Error bars indicate standard deviation of the results from three replicated biotic columns.

of magnitude in biochar and by two in GAC-amended columns. The optimized parameters indicated that GAC had the fastest adsorption and the highest sorption capacity for the polar vehicle-related organic pollutants we used.

Among the studied contaminants, DPG had the highest attachment rate coefficient in the three packing materials (9.47×10^{-3} , 3.15×10^{-2} , and $6.71 \times 10^{-2} \text{ min}^{-1}$ for columns filled with sand, biochar, and GAC, respectively) and the highest S_{max} in sand-only and biochar-amended columns (7.0 and 13.5 g^{-1} , respectively). BTZ had the highest S_{max} (276.8 g^{-1}) in GAC-amended columns. HMMM presented the lowest parameter values (k_a and S_{max}). The differences in the optimized attachment rate coefficients provided insight into the sorption affinity of the contaminants. HMMM, the least hydrophobic compound (Table 1), exhibited a low affinity to both PCM. BTZ and DPG exhibited a similar higher affinity in GAC and biochar. The same general trend was observed and discussed in the batch experiments (kinetics and screening).

The saturation of sorption sites modelled with the Langmuirian dynamics approach could be explained by the expected fouling effect caused by the excess of DOM in the system (DOC was approximately 5 mg C L^{-1} , typical stormwater range), which was likely intensified by the DOM preloading during conditioning (emulating a pre-conditioned operative field filter). The adsorption hindrance due to DOM fouling is well-known in water treatment applications with carbonaceous geomeedia (Teixidó et al., 2012; Boehm et al., 2020). Contaminant sorption could have been affected by DOM molecules either by direct sorption site competition or sorption site blockage, depending on their size (Li et al., 2003). This made it increasingly difficult for the contaminant molecules to sorb onto vacant adsorbent sites and may have led to even more rapid breakthroughs. Fouling probably affected HMMM, the largest compound (by molecular weight and van der Waals molecular volume; Table 1) most, since steric hindrance to diffusion and contaminant sorption reduction due to DOM presence can increase with molecular volume (Pignatello et al., 2006; Xiao et al., 2017). DOM was obtained from natural sources, and hence, the effects found on the adsorption of the contaminants could be considered representative for environmental systems.

In agreement with Li et al. (2003), the contaminant retention suppression by DOM decreased with the PCM specific surface area ($\text{N}_2 \text{ B.E.T. surface area}$: biochar $6.09 \text{ m}^2 \text{ g}^{-1}$; GAC $878 \text{ m}^2 \text{ g}^{-1}$), probably due to higher availability of sorption sites (i.e., higher S_{max} in GAC-containing columns: $49\text{--}277 \text{ g}^{-1}$). This may partially explain the difference in removal between GAC and WSP550 biochar, but further characterization of the sorbents (e.g., pore size distribution, point of zero charge) and DOM (e.g., concentration and composition) is needed. Furthermore, the adsorption kinetics experiment and the fitted transport parameters from the HYDRUS 1-D models underlined the faster adsorption kinetics in GAC. Thus, the higher surface area and the faster kinetics may have facilitated the contaminant removal in GAC amendments and led to significantly higher attenuation (i.e., reduction in the concentration of contaminants).

Overall, results suggested that the BTZ, DPG, and HMMM sorption mechanism onto the studied carbon-based materials mainly involved non-specific hydrophobic effects, together with specific interactions. BTZ, DPG, and HMMM aromatic rings could have interacted with the PCM polyaromatic sheets via $\pi\text{--}\pi$ EDA interactions (Kah et al., 2017). Electro-negative atoms (e.g., N and O) in the functional groups present in both contaminant and along the PCM edges of the graphene sheets could have interacted via coulombic and London–van der Waals forces, together with H-bonding interactions (Pignatello et al., 2017) and contributed to sorption. HMMM, the largest compound and the one with the lowest $\log K_{\text{OC}}$ values (Table 1), was the least retained contaminant, emphasizing the role of solute hydrophobicity and steric effects in the retention of the studied compounds. In contrast, BTZ and DPG, with higher $\log K_{\text{OC}}$ values (Table 1), may have had additional contributions to their sorption. BTZ, with the smallest molecular volume (Table 1), had the lowest steric hindrance to diffusion (size exclusion), and the cationic form of DPG ($\text{pK}_a = 9.38$) was likely assisted by the electrostatic attractive forces with the negatively charged PCM surfaces (Kah et al., 2017). These results

agree with Tang and Kolodziej (2022), where HMMM was found to be the most mobile compound in different natural soils and compost-amended sand, and its sorption process was not solely governed by hydrophobic effects. Nevertheless, complementary studies, including isotherms and evaluation of critical surface properties of sorbents (e.g., point of zero charge and functional groups by FTIR), are needed to elucidate adsorption mechanisms and better understand the PCM performance (Tong et al., 2019).

3.2.4. Simulation of service life

Operating at a continuous 5.5 cm h^{-1} flow rate regime and amended with 0.5 wt% of geomeedia, the material lifetime of a biofilter in Barcelona City was estimated to be 30 and 50 years for WSP550 biochar (1.9 mmol kg^{-1} reactive capacity) and GAC (3.2 mmol kg^{-1} reactive capacity), respectively. Both materials would likely be replaced prior to the end of their estimated service life (guidelines recommend periodic replacement around every ten years) (Grebel et al., 2013), and results indicated that much less PCM might be needed to maintain the removal of the studied pollutants. This example helps to illustrate the benefits of adding GAC and biochar to enhance the removal of polar vehicle-related organic contaminants in stormwater, even when long-term exposition to stormwater DOC is considered. However, these results should be interpreted cautiously, because projections derived from a 1-D model, assumed a negligible contaminant (bio)transformation, a continuous and steady stormwater inflow, a homogeneous media, and particulate-free synthetic stormwater. Field conditions are more complex, i.e., spatial and temporal variations in runoff composition, inflow intermittency, water flow velocity, transverse dispersion, the occurrence of dilution effects, channelling, clogging (physical, chemical and biological), organic carbon composition and concentration, and vegetation (plant roots create preferential flow paths) (Schijven and Šimůnek, 2002).

There is a need for urban stormwater treatment strategies (Feng et al., 2022; Hamel and Tan, 2022; Rødland et al., 2022) and to study the removal of PMT contaminants in conventional and geomeedia-amended biofilters (Spahr et al., 2020), especially of those expected to have a higher affinity with the liquid phase. Understanding BTZ, DPG, and HMMM rate-limited adsorption, and the DOM effects serves to improve the design of upgraded stormwater infiltration systems and the prediction of contaminant removal rates. The importance of this is further highlighted by the PMT properties of these contaminants and their transformation products. Additional studies on adsorption kinetics, isotherms, sorption competition, and transformation products are necessary to elucidate adsorption mechanisms and better understand vehicle-related organic contaminants removal.

4. Conclusions

The present study is the first to investigate the removal of specifically vehicle-related PMT substances, including the recently reported DPG and HMMM (potential precursor) together with BTZ, a more widely studied PMT substance highly abundant in traffic-impacted stormwater that it is known to pass through current water treatment technologies. Our results showed similar affinity between DPG and BTZ (both top priority PMT substances) to the evaluated biochar (WSP550) and GAC in batch and column experiments, being sorption likely contributed by additional specific interactions besides hydrophobic effects. In contrast, HMMM (PMT precursor) was the least adsorbed compound and could be challenging to remove in biofilters. All the contaminants exhibited nonequilibrium transport in sand-only, biochar- and GAC-amended columns and exhibited breakthrough curves with a steep initial rise leveling off to a plateau. This is typical for nonequilibrium interactions of chemicals and media with kinetic effects upon transport. Furthermore, the presence of DOM in these systems led to the saturation of favorable sorption sites (i.e., fouling) and an even more rapid breakthrough of the contaminants.

Overall, these results demonstrate PCM capability to adsorb the investigated contaminants, especially GAC. The larger surface area, faster sorption kinetics, and higher sorption capacity of GAC, compared to the WSP550 biochar, helped to alleviate the DOM inhibitory effects on the contaminants

sorption. The extrapolation of results and simulation of service life showed how both carbonaceous materials could enhance the tested vehicle-related organic stormwater contaminants removal and last for more than one decade in a 1-m biofilter, which fits with standard guidelines and recommendations for maintaining pollutant removal in bioswales used as stormwater control measures. Herein, biochar has still proved to be a cost-effective stormwater treatment option, but its reactivity towards the most mobile pollutants could be compromised. The number of studied vehicle-related PMT substances should be expanded, e.g., including compounds with lower hydrophobicity (lower log K_{OC} and log D_{OW}). Finally, our study motivates future work on PMT contaminant removal in upgraded green infrastructure systems.

CRediT authorship contribution statement

María Alejandra Cruz: Investigation, Conceptualization, Formal analysis, Writing – original draft, Visualization, Writing – review & editing. **Jiaqi Xu:** Investigation, Formal analysis. **Jan Willem Foppen:** Funding acquisition, Supervision, Conceptualization, Methodology, Visualization, Formal analysis, Writing – review & editing, Project administration. **Sandra Pérez:** Funding acquisition, Conceptualization, Methodology. **Enric Vázquez-Suñé:** Funding acquisition, Conceptualization. **Marc Teixidó:** Supervision, Funding acquisition, Conceptualization, Methodology, Resources, Formal analysis, Writing – review & editing, Project administration.

Data availability

Zenodo, DOI: 10.5281/zenodo.7975100.

Declaration of competing interest

The authors declare that they have no known competing financial interests or personal relationships that could have appeared to influence the work reported in this paper.

Acknowledgements

The present research was conducted at the Institute of Environmental Assessment and Water Research (IDAEA) from the Spanish National Research Council (CSIC) in Barcelona, Spain. MAC thanks the 'EU Erasmus + Programme by the European Commission for her scholarship to pursue EMJMD in Groundwater and Global Change - Impacts and Adaptation and IHE-Delft Institute for an advanced class fellowship. JX thanks the Ministry of Science and Innovation for her FPI grant (PRE2021-099072). MT was supported by the Beatriu de Pinós fellowship, funded by the Agency for Management of University and Research Grants (AGAUR; reference code: 2020BP00280). MTP also wants to thank the Severo Ochoa Grant CEX2018-000794-S funded by MCIN/AEI/10.13039/501100011033. We thank Jacobi Carbons – The Activated Carbon Applications Company (special thanks to R. Alonso) and the UK Biochar Research Centre (UKBRC) at the University of Edinburgh (special thanks to Dr. O. Mašek) for providing the activated carbon and the studied standard biochars, respectively. The authors appreciate considerable support from the IDAEA Groundwater and Hydrogeochemistry group members J. Bellés and J. Gutiérrez for their time and effort in building the experiment setup and analytical assistance.

Appendix A. Supplementary data

Supplementary data to this article can be found online at <https://doi.org/10.1016/j.scitotenv.2023.164264>.

References

Alhelou, R., Seiwert, B., Reemtsma, T., 2019. Hexamethoxymethylmelamine – a precursor of persistent and mobile contaminants in municipal wastewater and the water cycle. *Water Res.* 165, 114973. <https://doi.org/10.1016/j.watres.2019.114973>.

- Arp, H.P.H., Hale, S.E., 2019. REACH: Improvement of Guidance and Methods for the Identification and Assessment of PMT/vPvM Substances. Umweltbundesamt, Dessau-Roßlau (ISSN 1862-4804).
- Ashoori, N., Teixidó, M., Spahr, S., LeFevre, G.H., Sedlak, D.L., Luthy, R.G., 2019. Evaluation of pilot-scale biochar-amended woodchip bioreactors to remove nitrate, metals, and trace organic contaminants from urban stormwater runoff. *Water Res.* 154, 1–11. <https://doi.org/10.1016/j.watres.2019.01.040>.
- Batalini de Macedo, M., Nóbrega Gomes Júnior, M., Pereira de Oliveira, T.R., H. Giacomoni, M., Imani, M., Zhang, K., Ambrogi Ferreira do Lago, C., Mendiondo, E.M., 2021. Low impact development practices in the context of United Nations sustainable development goals: a new concept, lessons learned and challenges. *Crit. Rev. Environ. Sci. Technol.* 0, 1–44. <https://doi.org/10.1080/10643389.2021.1886889>.
- Boehm, A.B., Bell, C.D., Fitzgerald, N.J.M., Gallo, E., Higgins, C.P., Hogue, T.S., Luthy, R.G., Portmann, A.C., Ulrich, B.A., Wolfand, J.M., 2020. Biochar-augmented biofilters to improve pollutant removal from stormwater-can they improve receiving water quality? *Environ. Sci. Water Res. Technol.* 6, 1520–1537. <https://doi.org/10.1039/d0ew00027b>.
- Brusseau, M.L., Yan, N., Van Glubt, S., Wang, Y., Chen, W., Lyu, Y., Dungan, B., Carroll, K.C., Holguin, F.O., 2019. Comprehensive retention model for PFAS transport in subsurface systems. *Water Res.* 148, 41–50. <https://doi.org/10.1016/j.watres.2018.10.035>.
- Buhrman, D.L., Basic, C., Betherm, R.A., 2008. *Trace Quantitative Analysis by Mass Spectrometry*. John Wiley, West Sussex.
- Challis, J.K., Popick, H., Prajapati, S., Harder, P., Giesy, J.P., McPhedran, K., Brinkmann, M., 2021. Occurrences of tire rubber-derived contaminants in cold-climate urban runoff. *Environ. Sci. Technol. Lett.* 8, 961–967. <https://doi.org/10.1021/acs.estlett.1c00682>.
- Chen, J.S., Ho, Y.C., Liang, C.P., Wang, S.W., Liu, C.W., 2019. Semi-analytical model for coupled multispecies advective-dispersive transport subject to rate-limited sorption. *J. Hydrol.* 579, 124164. <https://doi.org/10.1016/j.jhydrol.2019.124164>.
- de Wilde, T., Mertens, J., Spanoghe, P., Ryckebaeck, J., Jaeken, P., Springael, D., 2008. Sorption kinetics and its effects on retention and leaching. *Chemosphere* 72, 509–516. <https://doi.org/10.1016/j.chemosphere.2008.02.053>.
- Ekka, S.A., Rujner, H., Leonhardt, G., Blecken, G., Viklander, M., Hunt, W.F., 2021. Next generation swale design for stormwater runoff treatment: a comprehensive approach. *J. Environ. Manag.* 279, 111756. <https://doi.org/10.1016/j.jenvman.2020.111756>.
- Eriksson, E., Baun, A., Scholes, L., Ledin, A., Ahlman, S., Revitt, M., Noutsopoulos, C., Mikkelsen, P.S., 2007. Selected stormwater priority pollutants - a European perspective. *Sci. Total Environ.* 383, 41–51. <https://doi.org/10.1016/j.scitotenv.2007.05.028>.
- Esfandiari, N., Suri, R., McKenzie, E.R., 2022. Competitive sorption of Cd, Cr, Cu, Ni, Pb and Zn from stormwater runoff by five low-cost sorbents: Effects of co-contaminants, humic acid, salinity and pH. *J. Hazard. Mater.* 423, 126938. <https://doi.org/10.1016/j.jhazmat.2021.126938>.
- Farré, M. I., Pérez, S., Kantiani, L., Barceló, D., 2008. Fate and toxicity of emerging pollutants, their metabolites and transformation products in the aquatic environment. *TrAC Trends Anal. Chem.* 27, 991–1007. <https://doi.org/10.1016/j.trac.2008.09.010>.
- Feng, W., Liu, Y., Gao, L., 2022. Stormwater treatment for reuse: current practice and future development – a review. *J. Environ. Manag.* 301, 113830. <https://doi.org/10.1016/j.jenvman.2021.113830>.
- Gibert, O., Hernández, M., Vilanova, E., Cornellà, O., 2014. *Guideline protocol for soil-column experiments assessing fate and transport of trace organics*. Demeau 3, 54.
- Giger, W., Schaffner, C., Kohler, H.P.E., 2006. Benzotriazole and tolyltriazole as aquatic contaminants. 1. Input and occurrence in rivers and lakes. *Environ. Sci. Technol.* 40, 7186–7192. https://doi.org/10.1021/ES061565J/SUPPL_FILE/ES061565JSI20061004_053835.XLS.
- Grebel, J.E., Mohanty, S.K., Torkelson, A.A., Boehm, A.B., Higgins, C.P., Maxwell, R.M., Nelson, K.L., Sedlak, D.L., 2013. Engineered infiltration systems for urban stormwater reclamation. *Environ. Eng. Sci.* 30, 437–454. <https://doi.org/10.1089/ees.2012.0312>.
- Guefelo, J.L., Wunsch, A., McCray, J., Stults, J.F., Higgins, C.P., 2020. Subsurface transport potential of perfluoroalkyl acids (PFAAs): column experiments and modeling. *J. Contam. Hydrol.* 233, 103661. <https://doi.org/10.1016/j.jconhyd.2020.103661>.
- Hamel, P., Tan, L., 2022. Blue-green infrastructure for flood and water quality management in Southeast Asia: evidence and knowledge gaps. *Environ. Manag.* 69, 699–718. <https://doi.org/10.1007/s00267-021-01467-w>.
- Hinnenkamp, V., Balsaa, P., Schmidt, T.C., 2022. Target, suspect and non-target screening analysis from wastewater treatment plant effluents to drinking water using collision cross section values as additional identification criterion. *Anal. Bioanal. Chem.* 414, 425–438. <https://doi.org/10.1007/s00216-021-03263-1>.
- Hossain, S.M.G., McLaughlan, R.G., 2021. Nonequilibrium 2, 4-DCP uptake onto pine chips from aqueous solutions. *Environ. Technol.* 42, 4057–4063. <https://doi.org/10.1080/09593330.2020.1744738>.
- Johannessen, C., Pamiš, J.M., 2021. Environmental modelling of hexamethoxymethylmelamine, its transformation products, and precursor compounds: an emerging family of contaminants from tire wear. *Chemosphere* 280, 130914. <https://doi.org/10.1016/j.chemosphere.2021.130914>.
- Johannessen, C., Helm, P., Metcalfe, C.D., 2021. Detection of selected tire wear compounds in urban receiving waters. *Environ. Pollut.* 287, 117659. <https://doi.org/10.1016/j.envpol.2021.117659>.
- Kah, M., Sigmund, G., Xiao, F., Hofmann, T., 2017. Sorption of ionizable and ionic organic compounds to biochar, activated carbon and other carbonaceous materials. *Water Res.* 124, 673–692. <https://doi.org/10.1016/j.watres.2017.07.070>.
- Lattao, C., Cao, X., Mao, J., Schmidt-Rohr, K., Pignatello, J.J., 2014. Influence of molecular structure and adsorbent properties on sorption of organic compounds to a temperature series of wood chars. *Environ. Sci. Technol.* 48, 4790–4798. <https://doi.org/10.1021/es405096q>.
- Li, Q., Snoeyink, V.L., Mariñas, B.J., Campos, C., 2003. Elucidating competitive adsorption mechanisms of atrazine and NOM using model compounds. *Water Res.* 37, 773–784. [https://doi.org/10.1016/S0043-1354\(02\)00390-1](https://doi.org/10.1016/S0043-1354(02)00390-1).

- Liu, Y.S., Ying, G.G., Shareef, A., Kookana, R.S., 2011. Biodegradation of three selected benzotriazoles under aerobic and anaerobic conditions. *Water Res.* 45, 5005–5014. <https://doi.org/10.1016/j.watres.2011.07.001>.
- Luthy, R.G., Sharvelle, S., Dillon, P., 2019. Urban stormwater to enhance water supply. *Environ. Sci. Technol.* 53, 5534–5542. <https://doi.org/10.1021/acs.est.8b05913>.
- Mao, M., Ren, L., 2004. Simulating nonequilibrium transport of atrazine through saturated soil. *Ground Water* 42, 500–508. <https://doi.org/10.1111/j.1745-6584.2004.tb02618.x>.
- Mašek, O., Buss, W., Sohi, S., 2018. Standard biochar materials. *Environ. Sci. Technol.* 52, 9543–9544. <https://doi.org/10.1021/acs.est.8b04053>.
- Müller, K., Hübner, D., Huppertsberg, S., Knepper, T.P., Zahn, D., 2022. Probing the chemical complexity of tires: identification of potential tire-borne water contaminants with high-resolution mass spectrometry. *Sci. Total Environ.* 802, 1–9. <https://doi.org/10.1016/j.scitotenv.2021.149799>.
- Peter, K.T., Tian, Z., Wu, C., Lin, P., White, S., Du, B., McIntyre, J.K., Scholz, N.L., Kolodziej, E.P., 2018. Using high-resolution mass spectrometry to identify organic contaminants linked to urban stormwater mortality syndrome in Coho Salmon. *Environ. Sci. Technol.* 52, 10317–10327. <https://doi.org/10.1021/acs.est.8b03287>.
- Pignatello, J.J., Kwon, S., Lu, Y., 2006. Effect of natural organic substances on the surface and adsorptive properties of environmental black carbon (char): attenuation of surface activity by humic and fulvic acids. *Environ. Sci. Technol.* 40, 7757–7763. <https://doi.org/10.1021/es061307m>.
- Pignatello, J.J., Mitch, W.A., Xu, W., 2017. Activity and reactivity of pyrogenic carbonaceous matter toward organic compounds. *Environ. Sci. Technol.* 51, 8893–8908. <https://doi.org/10.1021/acs.est.7b01088>.
- Ray, J.R., Shabtai, I.A., Teixidó, M., Mishael, Y.G., Sedlak, D.L., 2019. Polymer-clay composite geomeedia for sorptive removal of trace organic compounds and metals in urban stormwater. *Water Res.* 157, 454–462. <https://doi.org/10.1016/j.watres.2019.03.097>.
- Reemtsma, T., Berger, U., Arp, H.P.H., Gallard, H., Knepper, T.P., Neumann, M., Quintana, J.B., Voogt, P. De, 2016. Mind the gap: persistent and Mobile organic compounds - water contaminants that slip through. *Environ. Sci. Technol.* 50, 10308–10315. <https://doi.org/10.1021/acs.est.6b03338>.
- Rødland, E.S., Lind, O.C., Reid, M.J., Heier, L.S., Okoffo, E.D., Rauert, C., Thomas, K.V., Meland, S., 2022. Occurrence of tire and road wear particles in urban and peri-urban snowbanks, and their potential environmental implications. *Sci. Total Environ.* 824. <https://doi.org/10.1016/j.scitotenv.2022.153785>.
- Sandré, F., Huynh, N., Gromaire, M.C., Varrault, G., Morin, C., Moilleron, R., Le Roux, J., Garrigue-Antar, L., 2022. Road runoff characterization: ecotoxicological assessment combined with (non-)target screenings of micropollutants for the identification of relevant toxicants in the dissolved phase. *Water* 14. <https://doi.org/10.3390/w14040511>.
- Schijven, J.F., Šimůnek, J., 2002. Kinetic modeling of virus transport at the field scale. *J. Contam. Hydrol.* 55, 113–135. [https://doi.org/10.1016/S0169-7722\(01\)00188-7](https://doi.org/10.1016/S0169-7722(01)00188-7).
- Schulze, S., Zahn, D., Montes, R., Rodil, R., Quintana, J.B., Knepper, T.P., Reemtsma, T., Berger, U., 2019. Occurrence of emerging persistent and mobile organic contaminants in European water samples. *Water Res.* 153, 80–90. <https://doi.org/10.1016/j.watres.2019.01.008>.
- Seiwert, B., Klöckner, P., Wagner, S., Reemtsma, T., 2020. Source-related smart suspect screening in the aqueous environment: search for tire-derived persistent and mobile trace organic contaminants in surface waters. *Anal. Bioanal. Chem.* 412, 4909–4919. <https://doi.org/10.1007/s00216-020-02653-1>.
- Šimůnek, J., Šejna, M., Saito, M., Sakai, M., van Genuchten, M., 2018. *The HYDRUS-1D Software Package for Simulating the One-Dimensional Movement of Water, Heat, and Multiple Solutes in Variably-Saturated Media*.
- Spahr, S., Teixidó, M., Sedlak, D.L., Luthy, R.G., 2020. Hydrophilic trace organic contaminants in urban stormwater: occurrence, toxicological relevance, and the need to enhance green stormwater infrastructure. *Environ. Sci. Water Res. Technol.* 6, 15–44. <https://doi.org/10.1039/c9ew00674e>.
- Spahr, S., Teixidó, M., Gall, S.S., Pritchard, J.C., Hagemann, N., Helmreich, B., Luthy, R.G., 2022. Performance of biochars for the elimination of trace organic contaminants and metals from urban stormwater. *Environ. Sci. Water Res. Technol.* 8, 1287–1299. <https://doi.org/10.1039/d1ew00857a>.
- Tang, T., Kolodziej, E.P., 2022. Sorption and desorption of tire rubber and roadway-derived organic contaminants in soils and a representative engineered geomedium. *ACS ES&T Water* 2, 2623–2633. <https://doi.org/10.1021/acsestwater.2c00380>.
- Teixidó, M., Pignatello, J.J., Beltrán, J.L., Granados, M., Peccia, J., 2011. Speciation of the ionizable antibiotic sulfamethazine on black carbon (biochar). *Environ. Sci. Technol.* 45, 10020–10027. <https://doi.org/10.1021/es202487h>.
- Teixidó, M., Granados, M., Prat, M.D., Beltrán, J.L., 2012. Sorption of tetracyclines onto natural soils: data analysis and prediction. *Environ. Sci. Pollut. Res.* 19, 3087–3095. <https://doi.org/10.1007/s11356-012-0954-5>.
- Teixidó, M., Hurtado, C., Pignatello, J.J., Beltrán, J.L., Granados, M., Peccia, J., 2013. Predicting contaminant adsorption in black carbon (biochar)-amended soil for the veterinary antimicrobial sulfamethazine. *Environ. Sci. Technol.* 47, 6197–6205. <https://doi.org/10.1021/es400911c>.
- Teixidó, M., Charbonnet, J.A., LeFevre, G.H., Luthy, R.G., Sedlak, D.L., 2022. Use of pilot-scale geomeedia-amended biofiltration system for removal of polar trace organic and inorganic contaminants from stormwater runoff. *Water Res.* 226. <https://doi.org/10.1016/j.watres.2022.119246>.
- Tomczyk, A., Sokołowska, Z., Boguta, P., 2020. Biochar physicochemical properties: pyrolysis temperature and feedstock kind effects. *Rev. Environ. Sci. Biotechnol.* 19, 191–215. <https://doi.org/10.1007/s11157-020-09523-3>.
- Tong, Y., McNamara, P.J., Mayer, B.K., 2019. Adsorption of organic micropollutants onto biochar: a review of relevant kinetics, mechanisms and equilibrium. *Environ. Sci. Water Res. Technol.* 5, 821–838. <https://doi.org/10.1039/c8ew00938d>.
- Ulrich, B.A., Im, E.A., Werner, D., Higgins, C.P., 2015. Biochar and activated carbon for enhanced trace organic contaminant retention in stormwater infiltration systems. *Environ. Sci. Technol.* 49, 6222–6230. <https://doi.org/10.1021/acs.est.5b00376>.
- Ulrich, B.A., Loehnert, M., Higgins, C.P., 2017. Improved contaminant removal in vegetated stormwater biofilters amended with biochar. *Environ. Sci. Water Res. Technol.* 3, 726–734. <https://doi.org/10.1039/c7ew00070g>.
- Werner, D., Karapanagioti, H.K., Sabatini, D.A., 2012. Assessing the effect of grain-scale sorption rate limitations on the fate of hydrophobic organic groundwater pollutants. *J. Contam. Hydrol.* 129–130, 70–79. <https://doi.org/10.1016/j.jconhyd.2011.10.002>.
- Wiener, E.A., LeFevre, G.H., 2022. White rot fungi produce novel tire wear compound metabolites and reveal underappreciated amino acid conjugation pathways. *Environ. Sci. Technol. Lett.* <https://doi.org/10.1021/acs.estlett.2c00114>.
- Xiao, F., Pignatello, J.J., 2015. Interactions of triazine herbicides with biochar: steric and electronic effects. *Water Res.* 80, 179–188. <https://doi.org/10.1016/j.watres.2015.04.040>.
- Xiao, X., Ulrich, B.A., Chen, B., Higgins, C.P., 2017. Sorption of poly- and perfluoroalkyl substances (PFASs) relevant to aqueous film-forming foam (AFFF)-impacted groundwater by biochars and activated carbon. *Environ. Sci. Technol.* 51 (11), 6342–6635. <https://doi.org/10.1021/acs.est.7b00970>.
- Zhang, K., Randelovic, A., Page, D., McCarthy, D.T., Deletic, A., 2014. The validation of stormwater biofilters for micropollutant removal using in situ challenge tests. *Ecol. Eng.* 67, 1–10. <https://doi.org/10.1016/j.ecoleng.2014.03.004>.